

# Disinhibition Mediates a Form of Hippocampal Long-Term Potentiation in Area CA1

Jake Ormond\*, Melanie A. Woodin\*

Department of Cell & Systems Biology, University of Toronto, Toronto, Ontario, Canada

## Abstract

The hippocampus plays a central role in memory formation in the mammalian brain. Its ability to encode information is thought to depend on the plasticity of synaptic connections between neurons. In the pyramidal neurons constituting the primary hippocampal output to the cortex, located in area CA1, firing of presynaptic CA3 pyramidal neurons produces monosynaptic excitatory postsynaptic potentials (EPSPs) followed rapidly by feedforward (disynaptic) inhibitory postsynaptic potentials (IPSPs). Long-term potentiation (LTP) of the monosynaptic glutamatergic inputs has become the leading model of synaptic plasticity, in part due to its dependence on NMDA receptors (NMDARs), required for spatial and temporal learning in intact animals. Using whole-cell recording in hippocampal slices from adult rats, we find that the efficacy of synaptic transmission from CA3 to CA1 can be enhanced without the induction of classic LTP at the glutamatergic inputs. Taking care not to directly stimulate inhibitory fibers, we show that the induction of GABAergic plasticity at feedforward inhibitory inputs results in the reduced shunting of excitatory currents, producing a long-term increase in the amplitude of Schaffer collateral-mediated postsynaptic potentials. Like classic LTP, disinhibition-mediated LTP requires NMDAR activation, suggesting a role in types of learning and memory attributed primarily to the former and raising the possibility of a previously unrecognized target for therapeutic intervention in disorders linked to memory deficits, as well as a potentially overlooked site of LTP expression in other areas of the brain.

**Citation:** Ormond J, Woodin MA (2009) Disinhibition Mediates a Form of Hippocampal Long-Term Potentiation in Area CA1. PLoS ONE 4(9): e7224. doi:10.1371/journal.pone.0007224

**Editor:** Fabien Tell, The Research Center of Neurobiology - Neurophysiology of Marseille, France

**Received:** April 13, 2009; **Accepted:** September 8, 2009; **Published:** September 29, 2009

**Copyright:** © 2009 Ormond et al. This is an open-access article distributed under the terms of the Creative Commons Attribution License, which permits unrestricted use, distribution, and reproduction in any medium, provided the original author and source are credited.

**Funding:** This work was funded by a National Science and Engineering Research Council operating grant to M.W. and an NSERC PGS scholarship to J.O. The funders had no role in study design, data collection and analysis, decision to publish, or preparation of the manuscript.

**Competing Interests:** The authors have declared that no competing interests exist.

\* E-mail: jake.ormond@utoronto.ca (JO); m.woodin@utoronto.ca (MAW)

## Introduction

Plasticity of synaptic connections between neurons in the hippocampus is thought to play a central role in learning and memory. Synaptic plasticity can be induced by patterned electrical stimulation at a number of synapses in the hippocampus, including the excitatory synapses of the trisynaptic and direct entorhinal-CA1 pathways, as well as at certain excitatory onto interneuron synapses, and inhibitory onto pyramidal neuron synapses [see 1 for a review]. LTP of CA3-CA1 glutamatergic transmission has become the leading model of synaptic plasticity, in part because of its dependence on NMDAR activation [2], which provides a mechanism for associating pre- and postsynaptic action potential firing, and which is also required *in vivo* for hippocampal-dependent spatial and temporal learning [3–5].

An analysis of the literature on feedforward inhibition in CA1 suggests that plasticity at inhibitory synapses might also be able to play a role in regulating the efficacy of CA3-CA1 transmission. When presynaptic CA3 pyramidal fire, the EPSP recorded in CA1 is followed in less than 2 ms by a disynaptic IPSP [6] originating from basket cells targeting the somatic compartment [7]. This delay between EPSP and IPSP is only half as long as the rise time of unitary EPSPs evoked by single cell firing in CA3 [8]. Furthermore, feedforward inhibition has been shown to overlap with the rising phase of the EPSP in hippocampal slices from guinea pigs [9]. Thus, feedforward inhibition should reduce EPSP amplitude recorded at the soma, as demonstrated for unitary EPSPs between pairs of CA3 neurons [10]. It follows that disinhibition, if expressed at

feedforward synapses, would reduce the shunting of excitatory currents, leading to an increase in EPSP amplitude.

While a number of studies have reported the expression of activity-dependent reductions in strength at inhibitory synapses in area CA1 [11–14], plasticity specifically at the feedforward inhibitory synapses has never been demonstrated. The purpose of the present study was to determine if pairing-induced disinhibition at feedforward inhibitory synapses would alter the efficacy of CA3-CA1 excitatory transmission. Being careful not to directly stimulate inhibitory fibers (see Figure 1A and D, Figure S1) while making whole-cell recordings in hippocampal slices from 2 month old rats, we found that feedforward inhibition does indeed reduce EPSP amplitude, and that disinhibition at feedforward synapses, expressed as a depolarization of the reversal potential for GABA<sub>A</sub>R-mediated currents [14] contributes to the increase in EPSP amplitude seen during LTP expression. Furthermore, we found that disinhibition can produce LTP of Schaffer collateral-mediated transmission even under conditions in which classic LTP at glutamatergic synapses is not expressed. Taken together, our results suggest that plasticity of feedforward GABAergic synapses may play a similar role to classic LTP in memory encoding in the hippocampus.

## Materials and Methods

### Ethics statement

All rats were maintained on a 12 h light/dark cycle with food and water provided ad libitum. The Animal Studies Committee at the University of Toronto approved all experimental protocols.

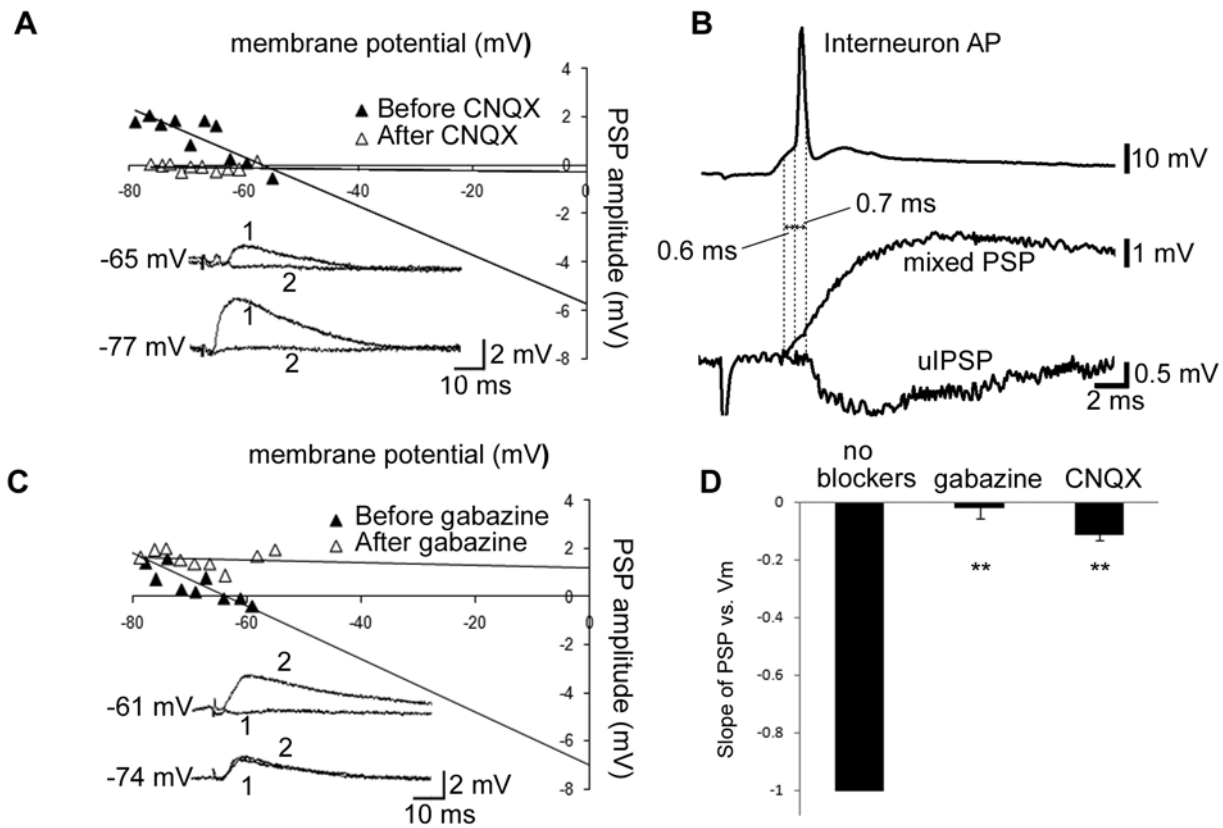


**Figure 1. Feedforward inhibition reduces EPSP amplitude.** **A**, PSP amplitude vs.  $V_m$  for one cell before and after CNQX. Inset: Sample traces before (1) and after (2) CNQX application. **B**, sample traces demonstrating the delay between the evoked pyramidal PSP and interneuron AP, and the delay between the interneuron AP and unitary IPSP (note that the intracellularly evoked interneuron AP, which produced the uIPSP, has been omitted for clarity). The PSP was recorded from a membrane potential of  $-82$  mV; the uIPSP was recorded from a membrane potential of  $-48$  mV. **C**, **left**, PSP amplitude vs.  $V_m$  for one cell before and after gabazine. Inset: Sample traces before (1) and after (2) gabazine application. **D**, The slope of the PSP vs.  $V_m$  graph before and after either gabazine ( $n=4$ ) or CNQX ( $n=29$ ), normalized to the before drug slope. \*\* denotes statistical significance from ctrl (no blockers; \*\*  $p<0.001$ ). Membrane potential denoted to left of sample traces in **A** and **C**.  
doi:10.1371/journal.pone.0007224.g001

### Brain slice preparation

400  $\mu$ m hippocampal slices were prepared from 50–75 day old (except where noted) male Sprague Dawley rats anesthetized with a mixture of ketamine and xylazine, and perfused through the ascending aorta with chilled modified artificial cerebrospinal fluid (ACSF). Modified ACSF was composed of 180 mM sucrose, 25 mM sodium bicarbonate, 25 mM glucose, 2.5 mM KCl, 1.25 mM sodium phosphate, 2 mM MgCl<sub>2</sub>, 1 mM CaCl<sub>2</sub>, 0.4 mM sodium ascorbate, and 3 mM sodium pyruvate, and saturated with 95% O<sub>2</sub>/5% CO<sub>2</sub> (pH 7.4, osmolarity  $\sim$ 305 mOsm). After cardiac perfusion, the brain was quickly removed, and hemispheres were separated and placed into the chilled solution for another 30 seconds. Hippocampi were then partially isolated by removing the cerebellum and all cortex except that directly overlying the hippocampus, to avoid damaging area CA1 while increasing the hippocampal surface area contacting oxygenated solution. The hippocampi were mounted vertically on an agar block and 400  $\mu$ m slices cut with a Vibratome 1000 plus. Slices recovered in 35–37°C ACSF composed of 125 mM NaCl, 25 mM glucose, 25 mM sodium bicarbonate, 2.5 mM KCl, 1.25 mM sodium phosphate, 1 mM MgCl<sub>2</sub>, and 2 mM CaCl<sub>2</sub> and saturated with 95% O<sub>2</sub>/5% CO<sub>2</sub> (pH 7.4, osmolarity  $\sim$ 305 mOsm) for 1 hour.

### Electrophysiology

Whole-cell recordings were made in oxygenated ACSF at 35–37°C from CA1 pyramidal cells, and in some experiments,

presynaptically connected feedforward interneurons. Pyramidal cells were identified by the presence of an after-depolarization following action potential firing, as well as action potential accommodation during prolonged AP trains. Feedforward interneurons were recorded in the pyramidal cell layer. Generally, we targeted cells that had much larger, and more irregularly shaped, cell bodies than the pyramidal cells. Their identity was confirmed electrophysiologically; they were excited to threshold by relatively low levels of Schaffer collateral stimulation (blocked by CNQX), and inhibited CA1 pyramidal neurons. Intracellular current injection always produced APs with large after-hyperpolarization; firing was always non-accommodating.

Whole-cell recording pipettes were pulled from thin-walled borosilicate (World Precision Industries, TW-150F) with a Sutter Instruments P-87 to resistances of 5–8 MOhms. Pipettes were filled with a solution consisting of 130 mM potassium gluconate, 10 mM KCl, 10 mM HEPES, 0.2 mM EGTA, 4 mM ATP, 0.3 mM GTP, 10 mM phosphocreatine (pH 7.25, osmolarity 275–285 mOsm). IPSPs recorded with this intracellular solution reversed at  $-88.3 \pm 1.6$  mV (LJP corrected;  $-74.3$  mV uncorrected;  $n=12$ ). This was nearly identical to the reversal recorded with gramicidin perforated patch ( $-88.5 \pm 1.2$  mV LJP corrected;  $-87$  uncorrected;  $n=6$ , data not shown), and there was no statistical difference between the two groups ( $p=0.673$ ). All membrane potential values in the text and figures are uncorrected

for the liquid junction potential. Signals were amplified using an Axon Instruments Multiclamp 700b and digitized using an Axon Instruments Digidata 1322a. The bridge was balanced upon going whole-cell, and then monitored and adjusted as necessary throughout the duration of recording.

Extracellular stimulation was applied through a whole-cell recording pipette containing a silver chlorided wire and filled with ACSF. The stimulus was generated by an AMPI ISO-Flex stimulus isolator triggered by an AMPI Master 8 stimulator, and was 100  $\mu$ sec in duration. The baseline recording frequency was 0.0333 Hz. Plasticity was induced by pairing extracellular stimulation with simultaneous current injection (1 nA for 10 ms) at 5 Hz (300 pairings; Figure 2A right inset shows an example pairing). For experiments examining LTP of mixed glutamatergic and GABAergic transmission, stimulation was applied to the Schaffer collaterals in CA3, so as to avoid the recruitment of monosynaptic inhibition in CA1 (Figure S1A). In experiments examining GABAergic plasticity, CNQX (10  $\mu$ M; Sigma) was applied to block AMPAR-mediated transmission, and the stimulating electrode was placed in stratum radiatum within 10–20  $\mu$ m of stratum pyramidale (Figure S1B). In experiments examining glutamatergic LTP, gabazine (6  $\mu$ M; Tocris) was applied to block GABA<sub>A</sub>R-mediated transmission, the CA3 region was cut away to prevent the generation of epileptic activity, and stimulation was applied in the Schaffer collaterals in CA1 (Figure S1C).

APV (25  $\mu$ M; Sigma), CNQX and gabazine were applied through bath perfusion, while AIP (5  $\mu$ M; Sigma) was applied through the patch pipette diluted in internal recording solution.

To determine the EPSP/feedforward IPSP delay, two measurements were made. First, the Schaffer collaterals were stimulated and the delay between the resulting PSP onset in the pyramidal neuron (determined visually) and the AP fired by the feedforward interneuron was measured. Second, AP firing in the interneuron was evoked with intracellular current injection, and the delay between the AP and the resulting postsynaptic unitary IPSP was measured (Figure 1B). These two delays were added to give the EPSP/feedforward IPSP delay.

To verify that the recorded inhibition was feedforward and not due to direct stimulation of inhibitory fibers, CNQX was perfused into the bath at the end of all mixed recordings. CNQX reduced the mean slope of the PSP vs. membrane potential relationship for all recordings by 89% (Figure 1D; Figure S2 displays this data for each individual experimental group). Because glutamatergic EPSPs make no significant contribution to the slope at the membrane potentials examined (Figure 1C, D), the reduction in slope after CNQX can be attributed to reduced inhibition.

## Data Analysis

Data was acquired using Axon Instruments Clampex 9 software, and analyzed using Axon Instruments Clampfit and Microsoft Excel. In all recordings, intracellular current steps were applied simultaneously with extracellular stimulation in sequences of 10, from the most negative to the most positive, so that PSP amplitude versus membrane potential graphs could be constructed in Microsoft Excel for each 5 min segment of the recording. For GABAergic recordings, the shift in the IPSP amplitude versus membrane potential graphs' x-intercept gave the change in  $E_{GABA}$ , while the change in slope provided the relative change in synaptic conductance. For mixed EPSP/IPSP recordings, the graphs were used to determine the average PSP amplitude from resting membrane potential (RMP; measured at the outset of each recording) for each 5 min segment. As EPSP amplitude showed no voltage dependence (Figure 1C, D), it was averaged for each 5 min segment to aid comparison with the other experimental groups.

## Statistics

Results are expressed as mean  $\pm$  s.e.m. All statistical tests were performed in Sigmapstat. Significance was determined using either a paired Student's t-test (Figure 1D, 3, S2) with significance level of  $P < 0.05$  or two-way repeated measures ANOVA (significance level of  $P < 0.05$ ) with post-hoc Tukey test (Figures 2, 4, 5, and 6; P values reflect the results of the post-hoc Tukey test). For all multiple comparisons in which statistical significance is reported, ANOVA values were significant to 0.05 or lower. EPSP 90% amplitude and rise time correlation was determined with linear regression.

## Results

To investigate the effect of feedforward inhibition on the amplitude of Schaffer collateral-mediated EPSPs, we stimulated the Schaffer collaterals close to their site of origin in CA3 (Figure S1A), and recorded mixed glutamatergic and GABAergic PSPs from pyramidal neurons in CA1. These PSPs were largely abolished by perfusion of the AMPA receptor (AMPA) antagonist CNQX (10  $\mu$ M; Figure 1A, D, Figure S2), indicating that inhibition was primarily elicited disynaptically. To determine whether the onset of feedforward inhibition was indeed rapid enough to reduce EPSP amplitude, we directly measured the EPSP-feedforward IPSP delay, previously found to be 1.9 ms in hippocampal slices from 1 month old Wistar rats recorded at 33°C [6]. To this end, we made paired recordings between synaptically connected feedforward interneurons (identified electrophysiologically; see Methods) and pyramidal cells. To calculate the EPSP-IPSP delay, the delay between the onset of the Schaffer collateral-evoked pyramidal cell EPSP and the interneuron AP ( $0.39 \pm .33$  ms,  $n = 10$ ) was added to the delay between the intracellularly-evoked interneuron AP and the resulting pyramidal unitary IPSP [ $0.90 \pm 0.07$  ms; same cells ( $n = 10$ ); Figure 1B]. This gave an EPSP-IPSP onset delay of  $1.3 \pm .3$  ms ( $n = 10$ ), much briefer than the mean rise time to 90% amplitude of pharmacologically isolated Schaffer collateral-evoked EPSPs [ $6.1 \pm .3$  ms; no correlation was observed between 90% amplitude (range = 0.5–4.5 mV) and rise time ( $r^2 = 0.00595$ ,  $p = 0.623$ ,  $n = 43$ ); data not shown]. This indicated that feedforward inhibition arrives in time to reduce EPSP amplitude. Moreover we found that membrane depolarization, which increases the driving force for  $Cl^-$  in the inward direction, has a strongly depressive effect on EPSP amplitude (Figure 1A, C; the mean reversal potential of mixed PSPs was  $-62.03 \pm 1.37$  mV,  $n = 22$ ). This depression of EPSP amplitude was completely blocked by the GABA<sub>A</sub> receptor (GABA<sub>A</sub>R) antagonist Gabazine (6  $\mu$ M), indicating that disynaptic inhibition elicited by Schaffer collateral-mediated glutamatergic transmission decreases the amplitude of EPSPs recorded at the soma.

We next examined how feedforward inhibition affects the magnitude of pairing-induced LTP. Pairing Schaffer collateral stimulation with postsynaptic spiking (300 pairings at 5 Hz; Experimental Procedures) produced a robust increase in mixed PSP amplitude (Figure 2A). However, when feedforward inhibition was blocked with gabazine, LTP was reduced (Figure 2B). The mere presence of feedforward inhibition would not be expected to enhance LTP, and has in fact been reported to instead diminish its magnitude [15]. We therefore suspected that a reduction in inhibitory strength induced by pairing was responsible for the enhanced LTP. To determine if this might be the case, we isolated inhibition pharmacologically with CNQX (NMDARs left unblocked), and paired extracellular stimulation close to the cell body layer (the site of feedforward synapses [7]) with postsynaptic spiking. This induced a depolarization of  $E_{GABA}$  (Figure 2C), as previously reported in hippocampal cultures and

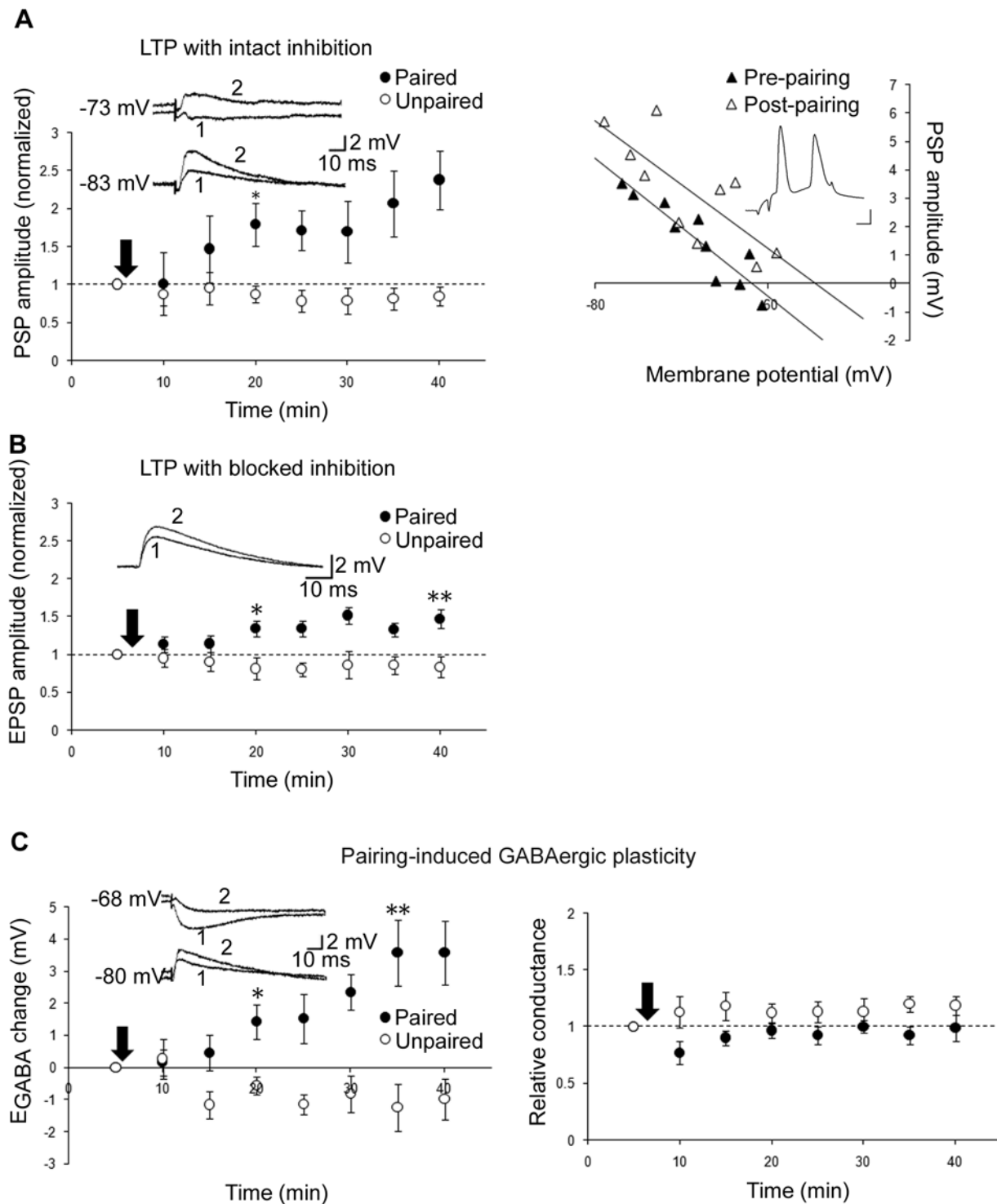


**Figure 2.  $E_{GABA}$  depolarization underlies a large component of mixed LTP.** **A**, Left: Mixed LTP (pairing  $n=6$ , ctrl  $n=5$ ). Inset: Sample traces before (1) and after (2) paired activity at two holding potentials. Right: Sample PSP vs. membrane potential plots for one cell before and 35 min after pairing. Inset: example of one pairing demonstrating timing of presynaptic stimulation and action potential firing. Scale bars: 20 mV, 2 ms. **B**, glutamatergic LTP (pairing  $n=7$ , ctrl  $n=5$ ; gabazine present throughout recording). Inset: Average of 10 traces before (1) and after (2) paired activity. **C**, GABAergic plasticity: change in  $E_{GABA}$  (left) and conductance (right; pairing  $n=6$ , ctrl  $n=5$ , same cells left and right; CNQX present throughout recording; NMDARs left unblocked). Inset: Sample traces before (1) and after (2) paired activity, at two holding potentials. \* and \*\* denote statistical significance from control ( $p<0.05$  and  $p<0.001$ , respectively) from that time point on. Arrows denote plasticity induction. doi:10.1371/journal.pone.0007224.g002

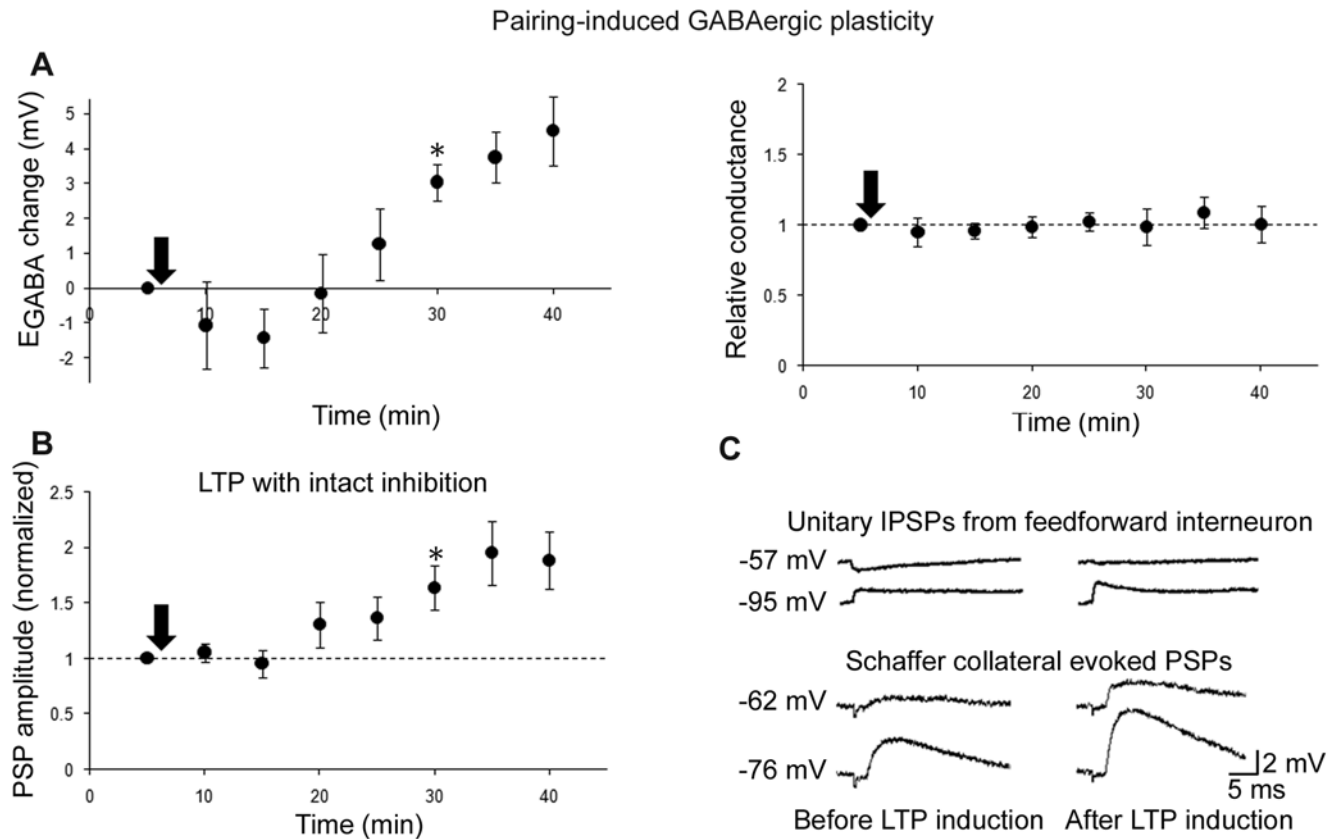


**Figure 3. LTP induction leads to simultaneous  $E_{GABA}$  depolarization and LTP.** **A**, GABAergic plasticity as determined by a depolarization of  $E_{GABA}$  (left) and no change in conductance (right). **B**, Mixed LTP with intact inhibition ( $n=7$ ). \*denotes statistical significance ( $p<0.05$ ) from that time point on. Arrows denote plasticity induction. **C**, sample traces of membrane potential from one cell at different holding potentials (denoted to left of sample traces).

doi:10.1371/journal.pone.0007224.g003

slices from juvenile rat [14]. Importantly, this also confirmed the previously reported observation that whole-cell recording does not interfere with the expression of pairing-induced GABAergic plasticity [14], which results from intracellular  $Cl^-$  accumulation due to a  $Ca^{2+}$  dependent down-regulation of the  $K^+/Cl^-$  cotransporter KCC2. No long-term changes in relative synaptic

conductance were observed (Figure 2C,  $p=0.173$ ). These results suggest that pairing-induced weakening of the GABAergic driving force increases the magnitude of LTP.

We next sought a direct confirmation that  $E_{GABA}$  depolarizes during LTP expression. To this end, we induced and monitored LTP with Schaffer collateral stimulation, while simultaneously

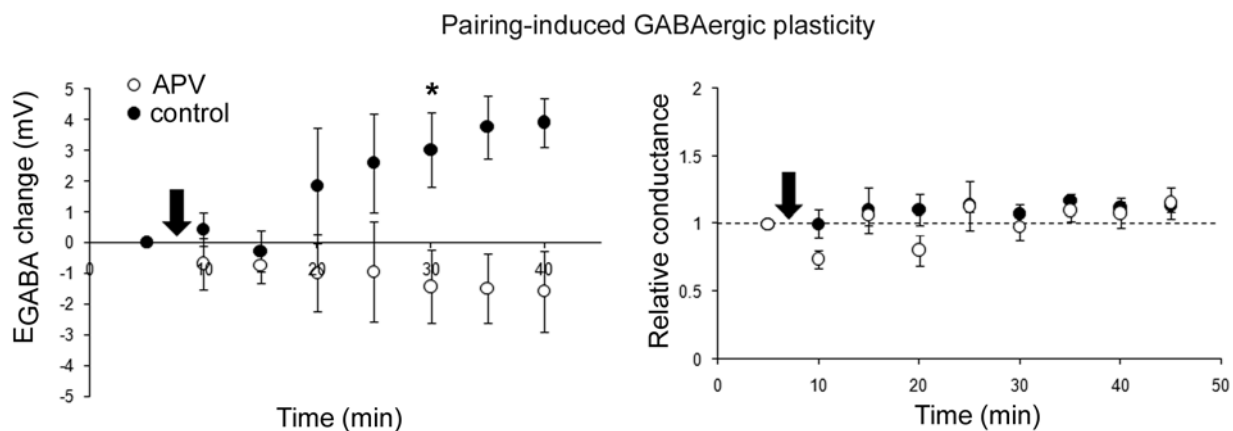


**Figure 4. APV blocks pairing-induced GABAergic plasticity.** GABAergic plasticity induced in the presence or absence of APV: change in  $E_{GABA}$  (left) and conductance (right; with APV  $n=5$ , without APV  $n=4$ , same cells left and right; CNQX present throughout recording). \* denotes statistical significance from control ( $p<0.05$ ) from that time point on. Arrows denote plasticity induction.

doi:10.1371/journal.pone.0007224.g004

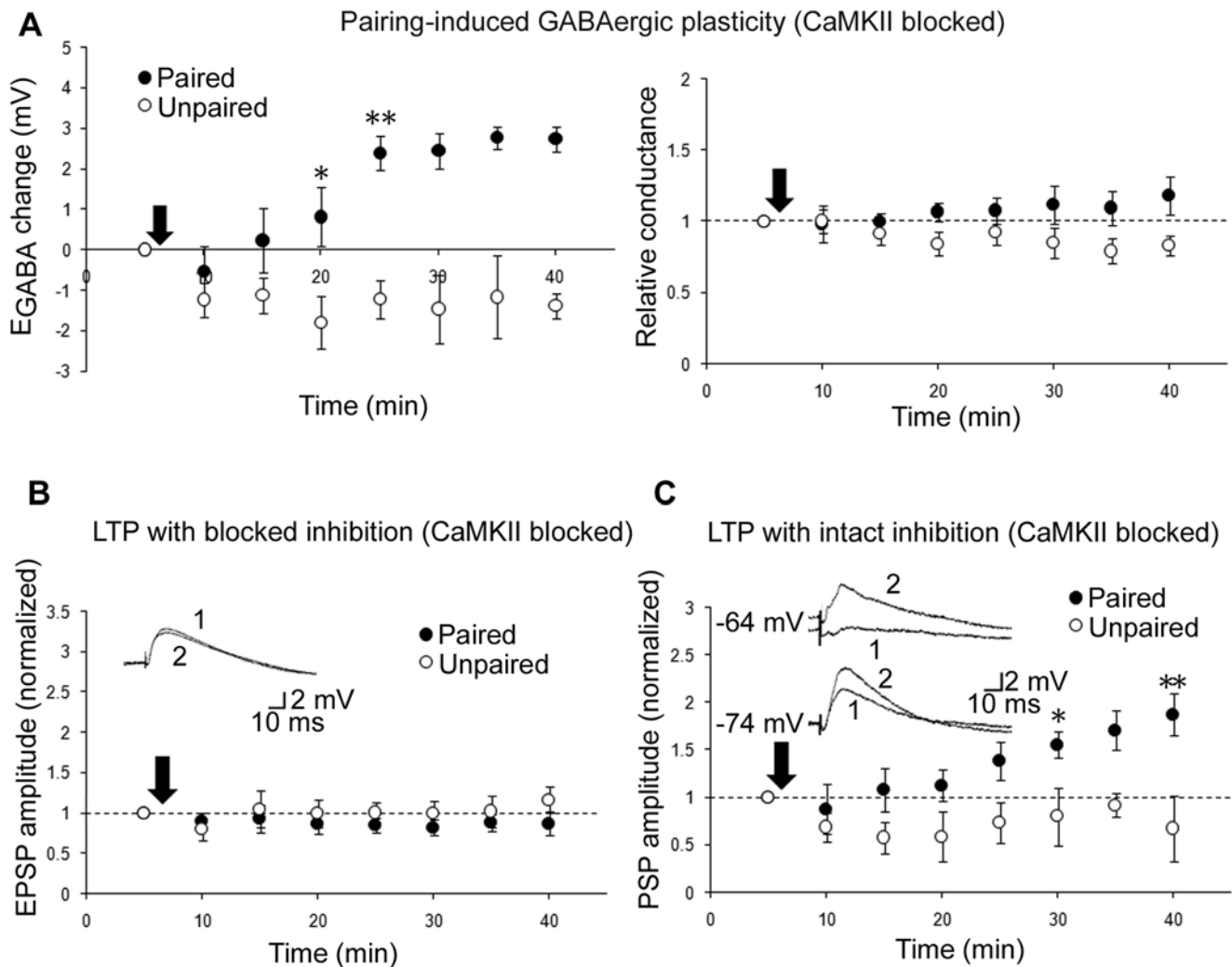


**Figure 5. Depolarization of  $E_{GABA}$  is sufficient for LTP expression.** **A**, GABAergic plasticity induced during CaMKII inhibition (change in  $E_{GABA}$  at left, conductance at right; pairing  $n=7$ , ctrl  $n=5$ , same cells left and right; CNQX present throughout recording, NMDARs left unblocked). Inset: Sample traces before (1) and after (2) paired activity. **B**, Glutamatergic LTP induced during CaMKII inhibition (pairing  $n=5$ , ctrl  $n=4$ ; gabazine present throughout recording). Inset: Average of 10 traces before (1) and after (2) paired activity. **C**, Mixed LTP induced during CaMKII inhibition (pairing  $n=6$ , ctrl  $n=5$ ). Insets: Sample traces before (1) and after (2) paired activity at two holding potentials (denoted to left of traces). CaMKII inhibitor AIP present in all recordings. \* and \*\* denote statistical significance from control ( $p<0.05$  and  $p<0.001$ , respectively) from that time point on. Arrows denote plasticity induction.

doi:10.1371/journal.pone.0007224.g005

monitoring  $E_{GABA}$  by evoking APs in a synaptically connected feedforward interneuron. Indeed, both  $E_{GABA}$  depolarization (Figure 3A, C) and LTP (Figure 3B, C) were expressed after pairing. Thus, pairing Schaffer collateral stimulation with pyramidal cell spiking induces a weakening of the driving force for GABAergic currents at feedforward synapses that contributes to LTP expression.

As a final confirmation of our results, we asked whether  $E_{GABA}$  depolarization alone would be sufficient to produce LTP. Our strategy was to block glutamatergic LTP pharmacologically with a drug that would leave pairing-induced inhibitory plasticity unaffected. Previous results had ruled out the involvement of NMDARs in pairing-induced inhibitory plasticity in slices from juvenile rats [14], making NMDAR blockers an attractive choice. However, given the possibility of developmental changes in the underlying mechanisms, as well as the fact that our stimulating electrode was positioned just outside of the cell body layer and therefore would have been simultaneously activating glutamatergic

synapses, we felt it prudent to test the effect of NMDAR blockade on pairing-induced  $E_{GABA}$  depolarization. Surprisingly, the NMDAR blocker APV (25  $\mu$ M) completely blocked both pairing-induced GABAergic plasticity (Figure 4) and LTP under conditions of intact inhibition (data not shown). We next tested inhibition of calcium/calmodulin-dependent protein kinase II (CaMKII), a  $Ca^{2+}$ -dependent kinase required for classic LTP induction [16]. Applying the CaMKII inhibitor autocamtide 2-related inhibitory peptide (AIP; 5  $\mu$ M; [17]) intracellularly through the patch pipette had no effect on inhibitory plasticity (Figure 5A; change in conductance  $p=0.078$ ), but abolished glutamatergic LTP when inhibition was blocked with gabazine ( $p=0.537$ , Figure 5B). When both inhibition and excitation were left intact, LTP induced by pairing was only slightly reduced by AIP (Figure 5C), as expected from the loss of the glutamatergic LTP component (Figure 2B). Thus, we conclude that disinhibition is sufficient to produce LTP of Schaffer collateral-mediated excitatory transmission.

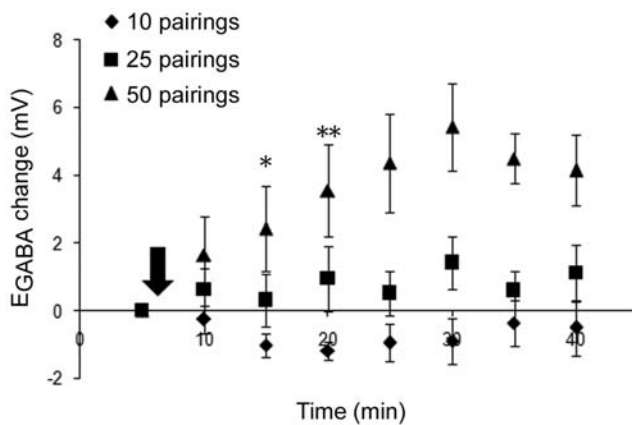


**Figure 6. Depolarization of  $E_{GABA}$  can be induced by as few as 50 pairings.** GABAergic plasticity induced by 10 pairings (diamond,  $n=7$ ), 25 pairings (square,  $n=6$ ), or 50 pairings (triangle,  $n=5$ ). CNQX present throughout recordings (NMDARs left unblocked). \* denotes statistical significance from Figure 2C control (\*  $<0.05$ , \*\*  $<0.001$ ; for statistical significance between groups see text) from that time point on. doi:10.1371/journal.pone.0007224.g006

Given the view that the hippocampal synaptic plasticity responsible for memory formation is thought to require only short periods of action potential firing [18], we wanted to know whether  $E_{GABA}$  depolarization could be induced by a briefer induction protocol. Leaving the frequency of stimulation unchanged, we examined the ability of 10, 25, or 50 pre- and postsynaptic pairings to induce plasticity (Figure 6). Neither 10 ( $p=0.74$ ) nor 25 ( $p=0.139$ ) pairings produced significant plasticity (no significant difference from control in Figure 2C), but 50 pairings produced a depolarization of  $E_{GABA}$  to a level indistinguishable from that induced by 300 pairings [ $p<0.001$  compared to control (Figure 2C) and 10 pairings,  $p=0.005$  compared to 25 pairings].

## Discussion

To our knowledge, this is the first report that long-term weakening of feedforward connections can augment the efficacy of Schaffer collateral-mediated glutamatergic transmission (see Figure S3 for model). We took great care to make sure that the inhibition being elicited was done in a way that was physiological so as to avoid overestimating the impact of inhibition on EPSP amplitude. By activating inhibitory inputs disynaptically rather than directly, we have maintained the physiological ratio of, and delay between, excitation and inhibition, and avoided the recruitment of interneuron types not involved in feedforward inhibition. Furthermore, under our whole-cell recording conditions, the driving force for  $GABA_A$ -mediated currents closely matched the driving force we measured with gramicidin perforated patch recording (see Materials and Methods), which leaves the intracellular  $[Cl^-]$  unperturbed. Lastly, we used slices from adult rats in all experiments. We believe the use of slices from adults is crucial for studying the cellular mechanisms underlying learning and memory, as ongoing neural development complicates the interpretation of data from younger animals. Highlighting this fact, we previously found that  $E_{GABA}$ , measured with gramicidin perforated-patch, hyperpolarizes a further 15 mV between 3 and 7 weeks of age [19] indicating that the developmental changes involved in strengthening inhibition extend into adolescence in the rat. As such, we think our study provides strong evidence of a role for disinhibition in LTP beyond the end of development, when synaptic plasticity is thought to primarily subservise the long-term storage of information.

A role for somatic disinhibition in E-S potentiation, the increase in postsynaptic excitability which normally accompanies classic LTP, has previously been reported [12–13]. Our data are consistent with a role for disinhibition in this phenomenon, but suggest that disinhibition-mediated E-S potentiation may result not from a change in the excitability of the postsynaptic neuron, but rather from increased somatic depolarization as a result of disinhibition at feedforward connections. This interpretation is entirely consistent with extracellular recording of E-S potentiation which shows a disproportionate enhancement of the population spike relative to the dendritic field potential [20–22], but will require a protocol capable of inducing disinhibition-mediated LTP without the need for pairing, which limits the disinhibition to a single neuron. It should be noted, however, that disinhibition is but one of a number of mechanisms underlying E-S potentiation, including relative changes in the ratio of excitation to inhibition due to glutamatergic LTP [23–24], as well as changes in intrinsic excitability expressed under conditions of pharmacological blockade of inhibition [25–29].

Interestingly, while the original demonstration of pairing-induced  $E_{GABA}$  depolarization in cell culture and slices from young rats (P11–19) found a requirement for  $Ca^{2+}$  influx through L-type  $Ca^{2+}$  channels rather than NMDARs [14], we instead found here that in slices from adult rats, NMDAR activation is required. This apparent developmental change in the source of  $Ca^{2+}$  required for  $E_{GABA}$  depolarization is supported by a recent report demonstrating the NMDAR-dependence of  $E_{GABA}$  depolarization induced in mature (DIV 19–22), but not young, cultures with bath perfusion of glutamate [30]. The same report also demonstrated that low-frequency stimulation of the Schaffer collaterals in 0%  $Mg^{2+}$  could induce NMDAR-dependent  $E_{GABA}$  depolarization in CA1 pyramidal cells of organotypic slices (prepared from P5–8, DIV 10–16). While it might seem unlikely that extracellular stimulation applied close to the cell body layer, as in our GABAergic plasticity experiments, would lead to NMDAR activation, synaptic NMDARs are in fact present all the way up the apical dendrite to the stratum pyramidale border [31–32]; due to the postsynaptic spiking induced during pairing, AMPAR-mediated depolarization would not have been required for the removal of their  $Mg^{2+}$  block. Candidate molecules and pathways involved in transducing NMDAR activation to KCC2 downregulation include PKC, required for the  $E_{GABA}$  depolarization induced by 5 minutes of postsynaptic spiking alone [33], and the BDNF-TrkB pathway, implicated by studies of the dramatic decrease in KCC2 expression following the kindling of seizures *in vivo* [34–35]. Whether the developmental changes in the activity-dependent regulation of KCC2 involve only the source of  $Ca^{2+}$ , or extend to the signalling pathways mediating this regulation is a question that will also need to be explored in future studies.

The lack of robust glutamatergic LTP in our experiments was beneficial in that it allowed us to more easily identify the contribution that disinhibition makes to LTP in the mixed EPSP/IPSP condition. Nevertheless, some might find this curious given the number of publications showing that paired pre- and postsynaptic activity, when separated with a positive (pre before post) spiking delay, produces robust glutamatergic LTP in CA1 pyramidal cells (eg. [36]). However, a number of publications have instead shown that such pairing induces either moderate LTP (eg. [37]), weak LTP (eg. [38]), or even long-term depression (LTD; [39]). There are a number of factors to consider when evaluating the effectiveness of a given induction protocol to induce glutamatergic LTP in addition to the pre-/postsynaptic delay: these include the number of pre- and postsynaptic spikes per pairing, the frequency of pairing, and the number of pairings. For example, while it is well

known that LTD can be induced by switching the order of pre- and postsynaptic pairing so that the postsynaptic firing occurs first [37,40], it can also be induced with pre- before post pairing if the number of pairings is greatly increased [39]. This can be partly understood due to the fact that both LTP and LTD require calcium influx through NMDARs (reviewed by [41]). Recent work has shed more light on this issue by showing that the processes underlying LTP and LTD can occur simultaneously, and that the resulting plasticity is due to the combinatory effects of these processes [42]. Given that LTP is normally induced by 50–100 pre-before post- pairings, and LTD requires approximately 900 such pairings, it is not surprising that our induction protocol consisting of 300 pairings, occupying the middle ground, induced only a weak glutamatergic LTP (though [38] reported a similar level of LTP induced with fewer pairings).

Our demonstration here that depolarization of  $E_{GABA}$  can be induced by both relatively low (50) and relatively high (300) numbers of pairings suggests that GABAergic plasticity may in some cases be co-expressed with glutamatergic LTP, and in other cases expressed in its absence. Pairing-induced LTP is hypothesized to modulate various aspects of place cell firing in the hippocampus, and possible examples of both low and high numbers of plasticity-inducing pairings can be found in the literature. For example, the experience-dependent expansion of place fields is induced by just a few passes through a given field [18]; this level of activity would be expected to induce both glutamatergic and GABAergic plasticity. Requiring more activity is the reactivation during sleep of neurons which co-fired during waking exploration [43]; this study reported that reactivation was most robust in those neurons which fired the most number of action potentials, across an examined range of 40–280, during exploration. As discussed above, increasing the number of pairings across this range would actually decrease the magnitude of glutamatergic LTP, suggesting that this phenomenon might depend solely on GABAergic plasticity, and might in fact be disrupted by the glutamatergic LTP induced with fewer pairings.

The glutamatergic LTP hypothesis of memory has been strengthened by demonstrations of LTP-like changes accompanying memory formation *in vivo* [44,45]. Does any such evidence exist for pairing-induced GABAergic plasticity? In fact,  $E_{GABA}$  depolarization has been demonstrated in CA1 pyramidal neurons of the dorsal hippocampus in slices cut from animals that had completed spatial memory acquisition in a water maze task [46]. In that study, no parallel changes in excitatory transmission were observed, suggesting that GABAergic plasticity alone might underlie some forms of memory. This possibility is supported by our demonstration here that disinhibition at feedforward connections is sufficient for LTP expression. Furthermore, the NMDAR-dependence of pairing-induced  $E_{GABA}$  depolarization suggests that it may be involved in forms of memory attributed until now solely to classic glutamatergic LTP [3–5].

## References

- Nelson SB, Turrigiano GG (2008) Strength through diversity. *Neuron* 60: 477–482.
- Harris EW, Ganong AH, Cotman CW (1984) Long-term potentiation in the hippocampus involves activation of N-methyl-D-aspartate receptors. *Brain Res* 323: 132–137.
- Morris RG, Anderson E, Lynch GS, Baudry M (1986) Selective impairment of learning and blockade of long-term potentiation by an N-methyl-D-aspartate receptor antagonist, AP5. *Nature* 319: 774–776.
- Tsien JZ, Huerta PT, Tonegawa S (1996) The essential role of hippocampal CA1 NMDA receptor-dependent synaptic plasticity in spatial memory. *Cell* 87: 1327–1338.
- Huerta PT, Sun LD, Wilson MA, Tonegawa S (2000) Formation of temporal memory requires NMDA receptors within CA1 pyramidal neurons. *Neuron* 25: 473–480.
- Pouille F, Scanziani M (2001) Enforcement of temporal fidelity in pyramidal cells by somatic feed-forward inhibition. *Science* 293: 1159–1163.
- Glickfeld LL, Scanziani M (2006) Distinct timing in the activity of cannabinoid-sensitive and cannabinoid-insensitive basket cells. *Nat Neurosci* 9: 807–815.
- Sayer RJ, Friedlander MJ, Redman SJ (1990) The time course and amplitude of EPSPs evoked at synapses between pairs of CA3/CA1 neurons in the hippocampal slice. *J Neurosci* 10: 826–836.
- Karnup S, Stelzer A (1999) Temporal overlap of excitatory and inhibitory afferent input in guinea-pig CA1 pyramidal cells. *J Physiol* 516: 485–504.
- Miles R (1990) Synaptic excitation of inhibitory cells by single CA3 hippocampal pyramidal cells of the guinea-pig *in vitro*. *J Physiol* 428: 61–77.
- Stelzer A, Simon G, Kovacs G, Rai R (1994) Synaptic disinhibition during maintenance of long-term potentiation in the CA1 hippocampal subfield. *Proc Natl Acad Sci U S A* 91: 3058–3062.

## Supporting Information

**Figure S1** The recording configurations. (A) The configuration for recording (R) mixed excitatory and feedforward inhibitory synaptic transmission. The stimulating electrode (S), consisting of a patch pipet with silver-chlorided wire inserted, was placed close to the site of origin of the Schaffer collaterals in CA3 so as to minimize the activation of monosynaptic inhibition in CA1. (B) The configuration for recording (R) pharmacologically isolated inhibitory transmission. The stimulating electrode (S) was placed in stratum radiatum immediately adjacent (within 10–20  $\mu$ m) to the cell body layer in order to stimulate somatic inhibitory synapses (which include feedforward synapses) without physically damaging pyramidal cell bodies. (C) The configuration for recording (R) pharmacologically isolated excitatory transmission. The CA3 region was cut away from the slice to avoid the generation of epileptic activity. Stimulation (S) was applied to the Schaffer collaterals in area CA1.  
Found at: doi:10.1371/journal.pone.0007224.s001 (1.17 MB TIF)

**Figure S2** The majority of recorded inhibition in mixed EPSP/IPSP recordings was feedforward. Relative conductance after CNQX for each experimental group. Relative conductance was taken as the slope of the PSP vs. Vm graph after CNQX application divided by the slope before application (see Fig. 1A for example). Experimental groups: 1, mixed LTP (Figure 2A); 2, mixed control (Figure 2A); 3, mixed LTP (paired recordings; Figure 3B); 4, mixed LTP with AIP (Figure 5C); 5, mixed control with AIP (Fig. 5C).  
Found at: doi:10.1371/journal.pone.0007224.s002 (0.20 MB TIF)

**Figure S3** Disinhibition can increase the efficacy of CA3-CA1 synaptic transmission in the absence of classic LTP expression. (A) The dominant theory of classic LTP is that it is expressed mainly as an increase in AMPAR insertion at the postsynaptic side of the Schaffer collateral synapses onto CA1 pyramidal neurons. Much of the excitatory current generated by Schaffer collateral transmission is shunted by temporally overlapping feedforward transmission, such that the depolarization measured at the soma is smaller than that generated at the site of excitatory transmission in the dendrites. (B) Disinhibition at the feedforward connections can also increase the efficacy with which presynaptic CA3 pyramidal cells excite their postsynaptic CA1 pyramidal targets. Increased intracellular  $[Cl^-]$  reduces the driving force for GABAergic currents, thereby reducing the shunt of excitatory current.  
Found at: doi:10.1371/journal.pone.0007224.s003 (1.07 MB TIF)

## Author Contributions

Conceived and designed the experiments: JO. Performed the experiments: JO. Analyzed the data: JO. Contributed reagents/materials/analysis tools: MW. Wrote the paper: JO MW.



12. Lu YM, Mansuy IM, Kandel ER, Roder J (2000) Calcineurin-mediated LTD of GABAergic inhibition underlies the increased excitability of CA1 neurons associated with LTP. *Neuron* 26: 197–205.
13. Chevaleyre V, Castillo PE (2003) Heterosynaptic LTD of hippocampal GABAergic synapses: a novel role of endocannabinoids in regulating excitability. *Neuron* 38: 461–472.
14. Woodin MA, Ganguly K, Poo MM (2003) Coincident pre- and postsynaptic activity modifies GABAergic synapses by postsynaptic changes in Cl<sup>-</sup> transporter activity. *Neuron* 39: 807–20.
15. Meredith RM, Floyer-Lea AM, Paulsen O (2003) Maturation of long-term potentiation induction rules in rodent hippocampus: role of GABAergic inhibition. *J Neurosci* 23: 11142–11146.
16. Malinow R, Madison DV, Tsien RW (1988) Persistent protein kinase activity underlying long-term potentiation. *Nature* 335: 820–824.
17. Ishida A, Kameshita I, Okuno S, Kitani T, Fujisawa H (1995) A novel highly specific and potent inhibitor of calmodulin-dependent protein kinase II. *Biochem Biophys Res Commun* 212: 806–812.
18. Mehta MR, Quirk MC, Wilson MA (2000) Experience-dependent asymmetric shape of hippocampal receptive fields. *Neuron* 25: 707–715.
19. Ormond J, Woodin MA (2006) Bidirectional spike-timing plasticity of GABA<sub>A</sub> receptor-mediated inhibition in the hippocampus. *Society for Neuroscience Annual Meeting Abstract* 133.3/C59.
20. Bliss TV, Gardner-Medwin AR (1973) Long-lasting potentiation of synaptic transmission in the dentate area of the unanaesthetized rabbit following stimulation of the perforant path. *J Physiol* 232: 357–374.
21. Bliss TVP, Lomo T (1973) Long-lasting potentiation of synaptic transmission in the dentate area of the anaesthetized rabbit following stimulation of the perforant path. *J Physiol* 232: 331–356.
22. Andersen P, Sundberg SH, Sveen O, Swann JW, Wigstrom H (1980) Possible mechanisms for long-lasting potentiation of synaptic transmission in hippocampal slices from guinea pigs. *J Physiol* 302: 463–482.
23. Abraham WC, Gustafsson B, Wigström H (1987) Long-term potentiation involves enhanced synaptic excitation relative to synaptic inhibition in guinea-pig hippocampus. *J Physiol* 394: 367–80.
24. Marder CP, Buonomano DV (2004) Timing and balance of inhibition enhance the effect of long-term potentiation on cell firing. *J Neurosci* 24: 8873–8884.
25. Hess G, Gustafsson B (1990) Changes in field excitatory postsynaptic potential shape induced by tetanization in the CA1 region of the guinea-pig hippocampal slice. *Neuroscience* 37: 61–69.
26. Asztely F, Gustafsson B (1994) Dissociation between long-term potentiation and associated changes in field EPSP waveform in the hippocampal CA1 region: an in vitro study in guinea pig brain slices. *Hippocampus* 4: 148–56.
27. Daoudal G, Hanada Y, Debanne D (2002) Bidirectional plasticity of excitatory postsynaptic potential (EPSP)-spike coupling in CA1 hippocampal pyramidal neurons. *Proc Natl Acad Sci U S A* 99: 14512–7.
28. Staff NP, Spruston N (2003) Intracellular correlate of EPSP-spike potentiation in CA1 pyramidal neurons is controlled by GABAergic modulation. *Hippocampus* 13: 801–5.
29. Campanac E, Daoudal G, Anki N, Debanne D (2008) Downregulation of dendritic I(h) in CA1 pyramidal neurons after LTP. *J Neurosci* 28: 8635–43.
30. Kitamura A, Ishibashi H, Watanabe M, Takatsuru Y, Brodwick M, et al. (2008) Sustained depolarizing shift of the GABA reversal potential by glutamate receptor activation in hippocampal neurons. *Neurosci Res* 62: 270–277.
31. Fritschy JM, Weinmann O, Wenzel A, Benke D (1998) Synapse-specific localization of NMDA and GABA(A) receptor subunits revealed by antigen-retrieval immunohistochemistry. *J Comp Neurol* 390: 194–210.
32. Janssen WG, Vissavajhala P, Andrews G, Moran T, Hof PR, et al. (2005) Cellular and synaptic distribution of NR2A and NR2B in macaque monkey and rat hippocampus as visualized with subunit-specific monoclonal antibodies. *Exp Neurol* 191: S28–44.
33. Fiumelli H, Cancedda L, Poo MM (2005) Modulation of GABAergic transmission by activity via postsynaptic Ca<sup>2+</sup>-dependent regulation of KCC2 function. *Neuron* 48: 773–86.
34. Rivera C, Li H, Thomas-Crusells J, Lahtinen H, Viitanen T, et al. (2002) BDNF-induced TrkB activation down-regulates the K<sup>+</sup>-Cl<sup>-</sup> cotransporter KCC2 and impairs neuronal Cl<sup>-</sup> extrusion. *J Cell Biol* 159: 747–52.
35. Rivera C, Voipio J, Thomas-Crusells J, Li H, Emri Z, et al. (2004) Mechanism of activity-dependent downregulation of the neuron-specific K-Cl cotransporter KCC2. *J Neurosci* 24: 4683–91.
36. Magee JC, Johnston D (1997) A synaptically controlled, associative signal for Hebbian plasticity in hippocampal neurons. *Science* 275: 209–213.
37. Nishiyama M, Hong K, Mikoshiba K, Poo MM, Kato K (2000) Calcium stores regulate the polarity and input specificity of synaptic modification. *Nature* 408: 584–588.
38. Hardie J, Spruston N (2009) Synaptic depolarization is more effective than back-propagating action potentials during induction of associative long-term potentiation in hippocampal pyramidal neurons. *J Neurosci* 29: 3233–3241.
39. Christie BR, Magee JC, Johnston D (1996) The role of dendritic action potentials and Ca<sup>2+</sup> influx in the induction of homosynaptic long-term depression in hippocampal CA1 pyramidal neurons. *Learn Mem* 3: 160–169.
40. Bi GQ, Poo MM (1998) Synaptic modifications in cultured hippocampal neurons: dependence on spike timing, synaptic strength, and postsynaptic cell type. *J Neurosci* 18: 10464–10472.
41. Bear MF, Malenka RC (1994) Synaptic plasticity: LTP and LTD. *Curr Opin Neurobiol* 4: 389–399.
42. Wittenberg GM, Wang SS (2006) Malleability of spike-timing-dependent plasticity at the CA3-CA1 synapse. *J Neurosci* 26: 6610–6617.
43. O'Neill J, Senior TJ, Allen K, Huxter JR, Csicsvari J (2008) Reactivation of experience-dependent cell assembly patterns in the hippocampus. *Nat Neurosci* 11: 209–215.
44. Gruart A, Muñoz MD, Delgado-García JM (2006) Involvement of the CA3-CA1 synapse in the acquisition of associative learning in behaving mice. *J Neurosci* 26: 1077–1087.
45. Whitlock JR, Heynen AJ, Shuler MG, Bear MF (2006) Learning induces long-term potentiation in the hippocampus. *Science* 313: 1093–7.
46. Gusev PA, Alkon DL (2001) Intracellular correlates of spatial memory acquisition in hippocampal slices: long-term disinhibition of CA1 pyramidal cells. *J Neurophysiol* 86: 881–99.